

Investigation of Age-Related Changes in Physiological Kinetic Tremor

MARIA FERNANDA S. ALMEIDA, GUILHERME L. CAVALHEIRO, ADRIANO A. PEREIRA,
and ADRIANO O. ANDRADE

Biomedical Engineering Laboratory, Faculty of Electrical Engineering, Federal University of Uberlândia, Campus Santa Mônica, Bloco 1E, Av. João Naves de Ávila, 2121, Uberlândia, Minas Gerais 38.408-100, Brazil

(Received 21 December 2009; accepted 7 June 2010; published online 23 June 2010)

Associate Editor Catherine Disselhorst-Klug oversaw the review of this article.

Abstract—Tremor is the most common movement disorder characterized by repetitive and stereotyped movements. Most investigations on tremor attempt to understand its relation to neuromuscular dysfunctions. Therefore, there is a lack of studies that aim to investigate the complex relation between the physiological tremor and aging, especially in kinetic conditions. In this context, the main motivation of this research was to quantify age-related changes in the kinetic tremor of clinically healthy individuals. For this, a number of features extracted from tremor activity, obtained from digitized drawings of Archimedes' spirals, were analyzed. In total, 59 subjects participated in the experiments. These individuals were divided into seven groups according to their ages and two types of analysis were carried out. First, the tremor activity of young and elderly adults was investigated by means of traditional features commonly used in tremor analysis, and secondly, linear discriminant analysis (LDA) was employed for the study of the correlation between age and tremor. The results showed significant statistical differences between the kinetic tremor activity of the young and elderly groups. Furthermore, it was found that LDA allowed for the estimate of a unique feature, so-called *LDA-value*, which showed to be linearly correlated with age.

Keywords—Aging, Tremor detection, Tremor analysis, Archimedes' spiral.

INTRODUCTION

Tremor is an involuntary, rhythmic, oscillatory movement of a body part that can be classified in many ways, depending on its etiology, phenomenology, frequency, and location.^{21,32}

Address correspondence to Adriano O. Andrade, Biomedical Engineering Laboratory, Faculty of Electrical Engineering, Federal University of Uberlândia, Campus Santa Mônica, Bloco 1E, Av. João Naves de Ávila, 2121, Uberlândia, Minas Gerais 38.408-100, Brazil. Electronic mail: nandasalmeida@yahoo.com.br, glcavalheiro@yahoo.com.br, a.alves.pereira@uol.com.br, aoandrade@feelt.ufu.br

A number of studies and governmental statistics have shown that the elderly population is the most affected by tremor and its consequences, which are responsible for physical limitations of these individuals.⁴ In this context, and also because of the increase in this population in many countries all over the world, studies that contribute to the understanding of tremor in the elderly are of paramount importance. One of the main difficulties of studying aging is that this phenomenon is based on demographic factors, which highlights the importance of understanding and comparing the results of research carried out all over the world.

The movement caused by tremor can be associated with factors such as neurological disorders and natural processes.^{8,10,32} The former is called pathological tremor, whereas the latter is often referred to as physiological tremor. The physiological tremor occurs normally in healthy individuals and, in general, it cannot be observed by the naked eye. However, some alterations and aggravations can amplify tremor making it visible, like stress situations, anxiety, muscular fatigue, and the use of certain drugs.^{5,32}

Most studies found in literature are related to the analysis of pathological tremor,^{1,8,10,12,13,15,17,20,24,28,30,35} highlighting the lack of investigations aiming to understand the complex relation between physiological tremor and aging, specifically in kinetic conditions.^{11,23,25,29,33}

The most common methods for measuring tremor are through the analysis of accelerometry and electromyography.^{10,11,25,29,33,34} Another common method to analyze it is by means of the study of hand-drawing movements.^{12,13,15,17,24,28,30,35} This kind of analysis makes possible the study of the kinetic tremor, which occurs during voluntary movement.

Many studies concerning the analysis of tremor and aging are based on specific populations and even specific households.^{2,3,18,19} This is because aging is a complex process that is influenced by genetic and demographical variables, such as quality of life, diet, and climate. Studies related to the understanding of physiological tremor in Brazil are scarce and this was an additional motivation for carrying out this research.

Hand-drawing patterns are commonly assessed by means of visual rating scales.^{20,23} However, such scales provide only crude subjective estimates of tremor amplitude. In order to reduce the subjectivity and limitation of some methods based on visual scales, there have been developed a few strategies for electronically measuring tremor, such as accelerometry and digitizing tablets. The use of digitizing tablets is common and provides the possibility of tremor activity detection under kinetic conditions.

The usual function of a digitizing tablet is to enable the analysis of drawings directly on the computer. The measurement of tremor by using digitizing tablets is a non-invasive alternative for tremor detection that combines simplicity with the precision and versatility of computational methods. The digitizing tablet is able to inform the position of the tip of the pen on its surface. By using this property this device can detect the movement of a subject following standard drawing patterns placed on it. In this study, the selected drawing pattern is the spiral of Archimedes as it is the gold-standard in neurological assessments.^{11–13,15,17,20,24,30,35}

Several attributes of the spiral of Archimedes make its use attractive in tests for the detection of human tremor. First, it has a simple design and it is easily understood by subjects who can follow its trajectory. Secondly, the shape of the spiral is smooth with an increasing radius, reducing the occurrence of false-positive tremor caused by abrupt changes in the direction of motion.

There are a number of research studies concerning the employment of digitizing tablets for both the quantification of pathological tremor and the detection of movement disorders.^{12–15,17,20,24,30,35} However, even with the advances in the technology of digitizing tablets, which allowed for more precision and accuracy in the measurement of movements, no study focusing upon the use of these devices, as a tool for investigating the relation between physiological tremor and aging in kinetic conditions, was found in our literature survey. Although some authors, e.g., Wenzelburger *et al.*,³⁶ support the hypothesis that kinetic tremor is related to an enhancement of physiological tremor this assumption is not consensual^{11,29,33} and therefore additional studies in this area are required.

In order to contribute to the understanding of age-related changes in physiological tremor under kinetic conditions, this study proposes to quantify tremor by means of the analysis of digitized hand-drawn drawings of clinically healthy individuals. For this, we employ a number of traditional features and also the linear discriminant analysis (*LDA*)-value, which is a feature based on *LDA* introduced by Cavalheiro *et al.*⁷ for postural control analysis.

MATERIALS AND METHODS

Criteria for Recruitment of Subjects and Definition of Groups

In total, 59 healthy subjects, i.e., without clinical evidences of suffering from any neurological disorder, as assessed by a neurologist, participated in our experiments. Prior to data collection the subjects signed a Consent Form approved by the Ethical Committee of the Federal University of Uberlândia, Brazil.

The subjects were divided into groups according to their ages, totaling seven groups, being: G1 = {20–29 years} ($N = 10$ subjects, seven males and three females), G2 = {30–39 years} ($N = 10$ subjects, eight males and two females), G3 = {40–49 years} ($N = 9$ subjects, six males and three females), G4 = {50–59 years} ($N = 8$ subjects, two males and six females), G5 = {60–69 years} ($N = 10$ subjects, three males and seven females), G6 = {70–79 years} ($N = 8$ subjects, two males and six females), and G7 = {80–89 years} ($N = 4$ subjects, two males and two females).

The number of subjects in the group G7 is relatively small when compared to the other groups in the analysis. This limitation, which can interfere in the reliability of the statistical analysis, is justified by difficulties in recruiting healthy individuals in our community in this age range (80–89 years old). Since one of the recruitment criteria of our study was to recruit healthy individuals without neurological impairments and who did not take medications that may increase or decrease tremor, we could not get enough subjects for the group G7 during the period of the research.^{13–15,17,23–25,28,33,35,36}

Task Definition

The subjects were asked to sit in a comfortable chair with their feet flat on the floor and with their back straight. The digitizing tablet was placed on a table properly positioned in front of the subjects. After verbal and written explanation about the exam the subjects were asked to draw two samples of a Spiral of Archimedes with their dominant hand. The arms of the

subjects were not supported during the execution of the task. The first sample was collected with the subject drawing the spiral from its center to its extremity (outgoing spiral—OS), whereas for the second sample the subject drew the spiral from its extremity to its center (ingoing spiral—IS). This procedure was repeated thrice for each subject. The subjects were asked to draw the spiral at their natural speed. The collected spirals were digitized at 64 Hz through a digitizing tablet (Trust, model TB-4200) with a resolution of 120 lines/mm.

Strategy for Data Analysis

Two types of analyses were carried out. First, we investigated differences in the tremor activity between young (formed by groups G1 and G2) and elderly groups (formed by groups G6 and G7) as normally found in other studies.^{11,25,33} Secondly, we considered the entire group of subjects from G1 to G7 in order to verify smoother changes that may happen with aging. The analyses followed, for each data sample, the sequence of steps below:

1. Linearization of the spiral of Archimedes;
2. Estimate of the tremor activity;
3. Data pre-processing;
4. Feature extraction from the tremor activity;
5. Estimate of the *LDA-value*.

Each of these steps is detailed below.

Linearization of the Spiral of Archimedes

The spiral of Archimedes is a geometrical shape that has a uniform distance between its turns equal to $2\pi b$. This kind of spiral can be represented by Eq. (1) in polar coordinates, where r is the radius, θ the angle, a and b are constants.

$$r = a + b\theta \quad (1)$$

The step of linearization consists in representing the original x and y coordinates of the spiral in terms of radius (r) and angle (θ) as shown in Eqs. (2) to (4).²⁸

$$x = r \sin(\theta) \quad (2)$$

$$y = r \cos(\theta) \quad (3)$$

$$r = \sqrt{x^2 + y^2} \quad (4)$$

The linearization of a perfect spiral results in a straightline as shown in Eq. (5) and depicted in Fig. 1, where m is the slope of the straightline.

$$r = m\theta \quad (5)$$

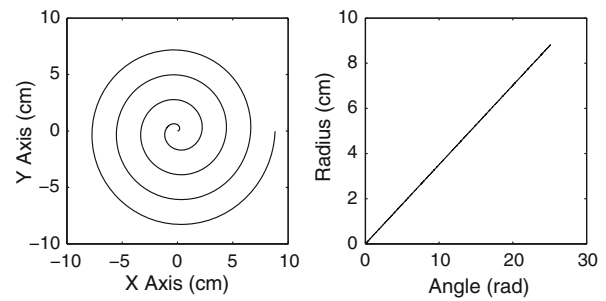


FIGURE 1. Illustration of the process of linearization of an ideal spiral of Archimedes. The spiral in the left panel is converted into a straightline in polar coordinates, which is shown in the right panel. This transformation eases the process of tremor estimate from hand-drawn spirals.

Although the linearization step does not offer any new information, it is extremely useful in the analysis of the spiral, as it is responsible for replacing the coordinates x and y by new ones, giving rise to a linear relationship between them.²⁸

Through this transformation, the mathematical computational operations become easier and faster, making it possible to analyze crucial aspects of the drawing of the spiral. When comparing the straightline obtained by means of the radius–angular transformation of the ideal spiral with that generated from an actual spiral, drawn by a subject, it is possible to detect irregularities.²⁸

Estimate of the Tremor Activity

The estimate of the tremor activity S is carried out by Eq. (6), where S_{ideal} is the ideal spiral (template) and S_{actual} is the spiral drawn by the subject.

$$S = S_{\text{ideal}} - S_{\text{actual}} \quad (6)$$

Figure 2 shows typical spirals obtained for the young and elderly subjects. In the figures the template spiral and its linearized version (Fig. 2b) are in black, whereas the actual spiral and its linearization are in red. The tremor activity S (Fig. 2c) is also presented for each case. Note that S is a random time-series and, therefore, it is possible to employ standard techniques for time-series analysis in order to extract information from it.

Data Pre-Processing

The tremor activity may be composed of (1) the inherent noise of the digitizing tablet, which is a low-frequency noise (<0.1 Hz) as suggested by the manufacturer; (2) voluntary movement whose energy is mostly limited to frequencies below 1 Hz^{15,17,35}; (3) and the specific-task physiological tremor which is

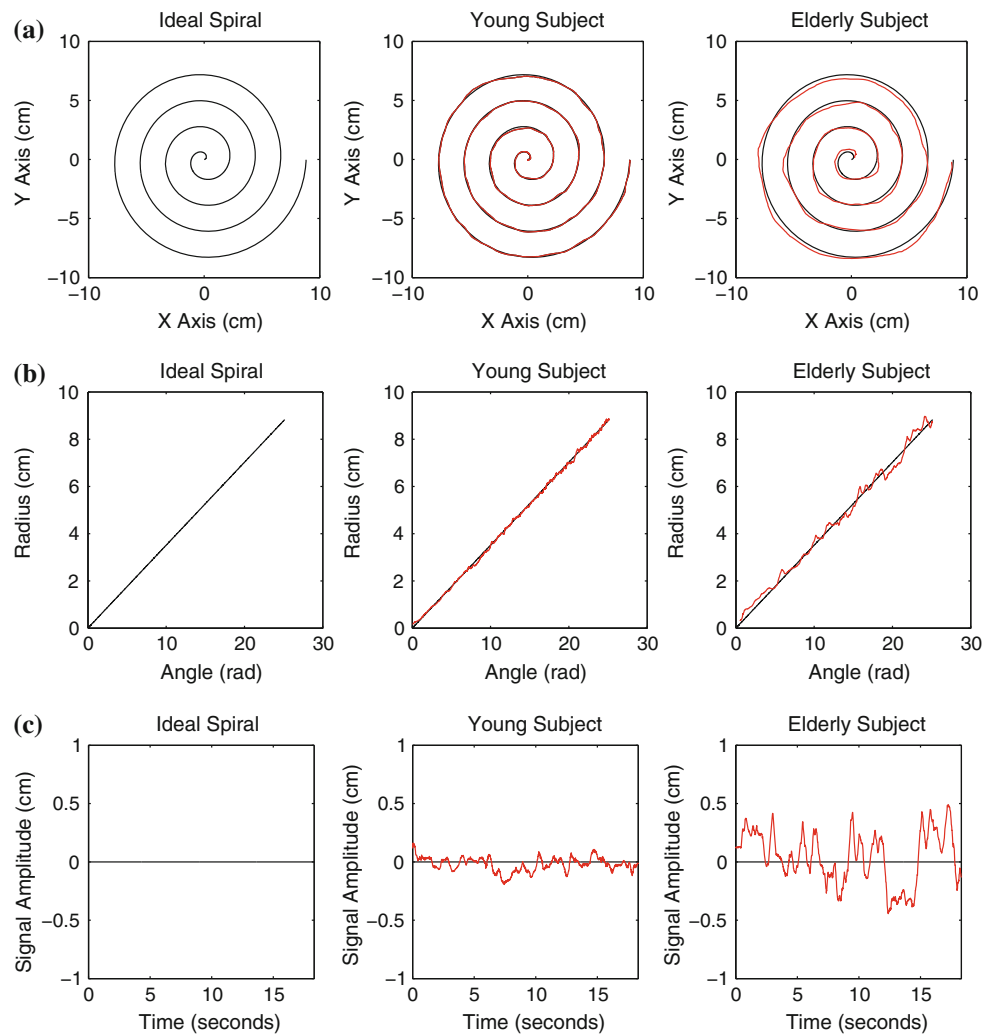


FIGURE 2. Example of the application of the process of linearization for an ideal spiral and two typical patterns obtained from hand-drawn spirals of young and elderly subjects. (a) The spiral drawn by each subject is compared against the ideal spiral. (b) The system coordinates are converted into polar coordinates and the results of each subject are contrasted to the ideal straightline, which represents the spiral in polar coordinates. (c) The tremor activity obtained for each subject is shown. This activity is obtained by subtracting the ideal spiral from the hand-drawn spiral in polar coordinates.

characterized by involuntary movements and energy mostly between 4 and 10 Hz.^{4,12,14,24,28,32} According to Elble *et al.*,¹² the acts of writing and drawing constrict the range of tremor frequencies. Methods such as accelerometry and electromyography do not offer a resistance like in the acts of writing and drawing, where there is a contact of the pen with the surface of the digitizing tablet. This means that distinct methods for tremor measurement may result in collected signals with different frequency and amplitude range.^{25,29,34}

As the main focus of this study is to investigate the specific-task physiological tremor it makes sense to limit the bandwidth of the signal to the range of interest as suggested in other investigations.^{15,17,36} Therefore, we applied a linear filter in order to obtain the physiological tremor activity for analysis. This

activity was filtered by using a fourth-order digital band-pass Butterworth filter. As the frequency response of the filter is not ideal we set its lower and upper cutoff frequencies to 2.5 and 20 Hz with the aim of preserving the bandwidth of interest. This bandwidth was carefully defined to capture the full-tremor component in task-specific physiological tremor, typically in the frequency range between 4 and 10 Hz,^{4,12,14,24,28,32} and also to avoid major influence of voluntary movements whose energy is normally concentrated in frequencies below 1 Hz.^{15,17,35}

Frequency analysis (energy estimate) was performed on the filtered signal by using the Welch's method with a 32-data point Hanning window.

Figure 3 illustrates the signal before and after filtering. Figures 3a and 3b show, respectively, typical

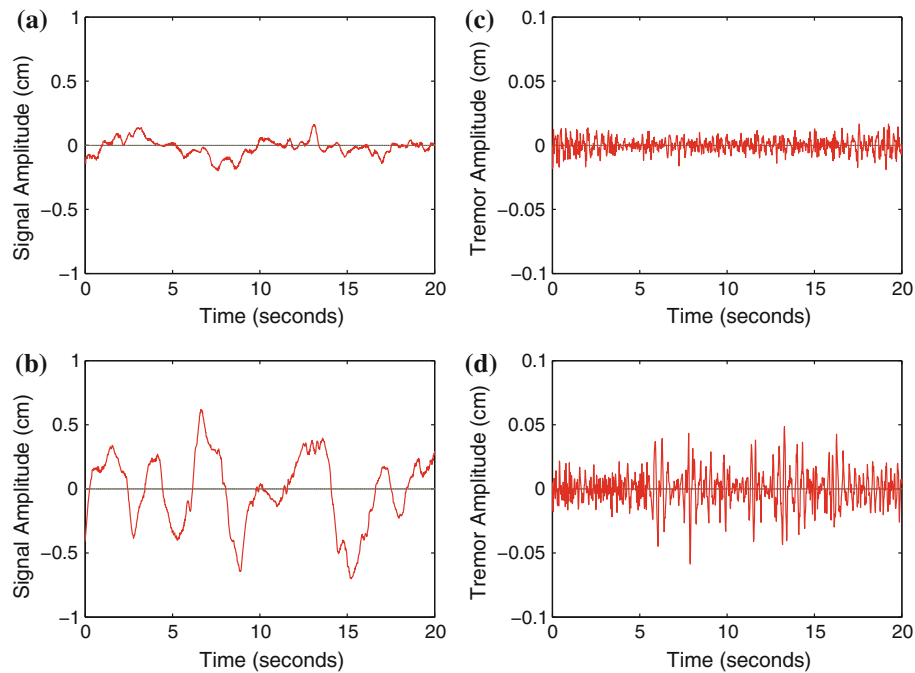


FIGURE 3. Illustration of the effect of filtering applied to typical collected signals from young (a, c) and elderly (b, d) adults. The non-filtered signals are depicted in (a, b), whereas their filtered versions are depicted in (c, d), respectively.

signals collected from a young and an elderly adult before filtering. Figures 3c and 3d are filtered versions of the signals shown in Figs. 3a and 3b, respectively. The waveform depicted in Fig. 3d shows an increase in amplitude when compared to the one in Fig. 3c. This increase in amplitude may be related to intermittent path corrections that could be modulated by tremor activity, which is larger in the elderly adult.

Feature Extraction From the Tremor Activity

In order to assess and quantify the tremor activity a number of traditional features described in the Appendix and listed in Table 4 were used. The description of the *LDA-value* follows below.

The *LDA-Value*

In addition to the traditional features we also employed a method inspired in LDA, which is a known method for data classification and dimensionality reduction. The main strategy of LDA is to assume that groups or classes are linearly separable and thus it is possible to estimate new features projected on optimized axes that maximizes the separability between classes. Specifically, LDA seeks a transformation matrix that maximizes the ratio of the between-class scatter to the within-class scatter.¹⁶

The technique employed in our study follows that described by Cavalheiro *et al.*⁷ for the estimate of the *LDA-value*, which is a one-dimensional variable,

estimated from the linear projection of features onto an optimized axis that maximizes class separability. Different from LDA, which basically uses the mean and covariance matrices of the classes for finding optimized axes, the technique used here employs genetic algorithm (GA) that is a search method used in computing to find solutions to optimization problems.³¹ The use of GA, although computationally expensive, does not assume the nature of the probability distribution function of the data.⁷ This technique has been successfully employed in a recent study concerning the relation between postural control and aging,⁷ and this was one of the main motivations for employing it in the context of tremor analysis. Furthermore, the possibility of obtaining a feature in a one-dimensional space, whenever possible, is relevant for easing the interpretation and visualization of results.

Figure 4 depicts a block diagram with the main steps required for the estimate of the *LDA-value*. The input to the algorithm is a data matrix (C_0) whose dimension is $m \times n$, where m is the number of multidimensional data points and n is the number of features.

Table 1 lists the description of the parameters employed for the estimate of the *LDA-value*.

The first step of the procedure consists in normalizing the matrix C_0 in order to avoid the influence of one feature upon another. Each feature (column of the matrix C_0) is normalized between 0 and 1, and an offset of 0.1 is added to the normalized matrix (C_N) for

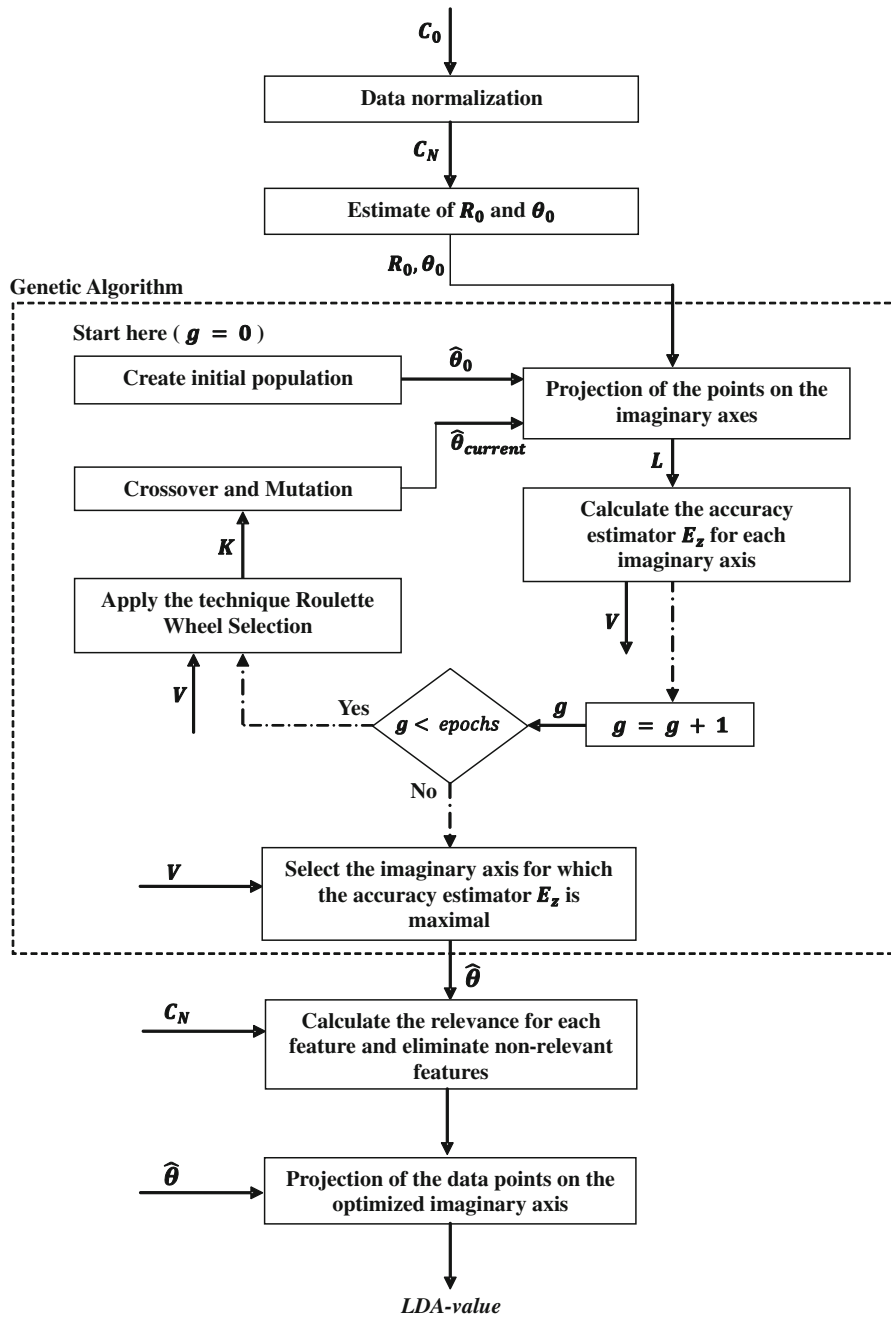


FIGURE 4. Block diagram depicting the main steps involved in the estimate of the *LDA-value*. The steps carried out by the application of GA are in the dotted box. The dotted arrows indicate that the application of the procedure is an iterative process controlled by a dummy variable (g). The description of the variables and sequence of the steps shown in the diagram are provided in the text.

avoiding division by zero when applying future signal processing stages.

The next step is related to the representation of the data (C_N) in multidimensional angular coordinate space as shown in Eqs. (7)–(9), where r is the radius and θ the angle. With this transformation it is possible to project the data onto a particular axis as shown in Eq. (10) yielding a single scalar, p , or a new

feature, which is a linear combination of the old ones. The main goal of the GA employed here is to find rotation angles, $\hat{\theta}_1, \hat{\theta}_2, \dots, \hat{\theta}_{n-1}$, which maximizes class separability. Note that initially Eqs. (7)–(9) should be applied to each row of the matrix C_N , yielding the parameters R_0 and θ_0 in \mathcal{R}^m . In addition, the application of Eq. (10) to optimized angles yields the *LDA-value*.⁷

TABLE 1. Description of the parameters employed for the estimate of the LDA-value.

Parameter	Dimension	Value	Description
C_0	59×36		Data matrix
C_N	59×36		Normalized data matrix
R_0	59		Radius for each data point
θ_0	59×35		Angle for each data point
$\hat{\theta}_0$	50×35		Initial population of the GA procedure
L	50×59		Projection of the data points on the imaginary axes
V	50		Set of the fitness function values for each imaginary axis
K	50×35		Population of imaginary axes selected through the technique Roulette Wheel Selection
$\hat{\theta}_{\text{current}}$	50×35		Population of imaginary axes obtained after crossover and mutation
$epochs$	1	50,000	Number of epochs
$\hat{\theta}$	35		Angle of the imaginary axis which has the maximal accuracy estimator
m	1	59	Number of multidimensional data points
n	1	36	Number of features
s	1	50	Number of individuals in the initial population
ξ	1	7	Number of classes
P_{mutation}	1	0.1	Probability of mutation
$P_{\text{crossover}}$	1	0.8	Probability of crossover

$$r = \sqrt{C_1^2 + C_2^2 + C_3^2 + \dots + C_n^2} \tag{7}$$

$$\theta = \{\theta_1, \theta_2, \theta_3, \dots, \theta_{n-1}\} \tag{8}$$

$$\begin{aligned} \theta_1 &= \tan^{-1}\left(\frac{C_2}{C_1}\right); \quad \theta_2 = \tan^{-1}\left(\frac{C_3}{\sqrt{C_1^2 + C_2^2}}\right); \\ \theta_3 &= \tan^{-1}\left(\frac{C_3}{\sqrt{C_1^2 + C_2^2 + C_3^2}}\right); \dots; \\ \theta_{n-1} &= \tan^{-1}\left(\frac{C_n}{\sqrt{C_1^2 + \dots + C_{n-1}^2}}\right) \\ p &= r * \cos(\theta_1 + \hat{\theta}_1) * \cos(\theta_2 + \hat{\theta}_2) \\ &\quad * \dots * \cos(\theta_n + \hat{\theta}_{n-1}) \end{aligned} \tag{9}$$

The application of GA starts with the definition of an initial population $\hat{\theta}_0$, of size s , which is carried out by sampling imaginary axes from the uniform distribution of a random variable whose possible values range from 0 to 2π . The matrix $\hat{\theta}_0$ has dimension $s \times (n - 1)$. In this step, a dummy variable (g) is set to zero and used as a counter in the iterative process, which stops when the number of pre-defined *epochs* is reached. Note that $\hat{\theta}_0$ is only used when $g = 0$ and that a newly updated (optimized) population $\hat{\theta}_{\text{current}}$ will be employed in the following iterations.

The procedure follows by projecting the multidimensional data set onto a one-dimensional space as

given by Eq. (10), resulting in the matrix L whose dimension is $s \times m$. The set of projections in L is used for the calculation of the accuracy estimator E_z as in Eq. (11), where ξ is the number of classes, \bar{x}_i and $\sigma_{x_i}^2$ are the mean and the variance of the i th class, \bar{x}_j and $\sigma_{x_j}^2$ are the mean and the variance of the j th class.

$$E_z = \sum_{i=1}^{\xi-1} \sum_{j=i+1}^{\xi} \left| \frac{(\bar{x}_i - \bar{x}_j)}{\sqrt{\sigma_{x_i}^2 + \sigma_{x_j}^2}} \right|, \quad z = 1, 2, \dots, s \tag{11}$$

The larger the value of the accuracy estimator E_z , the better will be the discrimination between classes. The main aim of GA is to seek rotation angles, for which E_z is maximal. In this step the set of E_z , which is the fitness function of the GA, is calculated for each imaginary axis resulting in the vector V shown in Eq. (12), and then the dummy variable g is increased. If the value of g is less than *epochs* the search procedure continues.

$$V = \begin{bmatrix} E_{z=1} \\ E_{z=2} \\ \vdots \\ E_{z=s} \end{bmatrix} \tag{12}$$

The next step is the application of the roulette-wheel selection, a sampling with replacement method commonly used in GA.⁶ The main idea of this process is to stochastically select from one generation to create the basis of the next generation. This selection procedure is based on selecting individuals of the population $\hat{\theta}_{\text{current}}$ taking into account their probability which is proportional to the respective value of E_z , and it will result the matrix K with dimension $s \times (n - 1)$.

The procedures of crossover and mutation are then applied to the population \mathbf{K} with probabilities $p_{\text{crossover}}$ and p_{mutation} . In crossover, portions of two parents ($\hat{\theta}_{\text{parent1}}$ and $\hat{\theta}_{\text{parent2}}$), from the current generation, are combined to create two offspring according to the heuristic crossover technique defined by Wright.³⁷ This method consists in the generation of three children ($\hat{\theta}_{\text{child}_1}$, $\hat{\theta}_{\text{child}_2}$, and $\hat{\theta}_{\text{child}_3}$) given by Eqs. (13)–(15) where only the two best children are selected according to the fitness function (E_z).

$$\hat{\theta}_{\text{child}_1} = 1.5\hat{\theta}_{\text{parent1}} - 0.5\hat{\theta}_{\text{parent2}} \quad (13)$$

$$\hat{\theta}_{\text{child}_2} = 0.5\hat{\theta}_{\text{parent1}} + 0.5\hat{\theta}_{\text{parent2}} \quad (14)$$

$$\hat{\theta}_{\text{child}_3} = -0.5\hat{\theta}_{\text{parent1}} + 1.5\hat{\theta}_{\text{parent2}} \quad (15)$$

Regarding the mutation process, a low probability of mutation (p_{mutation}) is allowed. When it happens, a single rotation angle of some individuals of \mathbf{K} will be randomly modified generating, therefore, a new population ($\hat{\theta}_{\text{current}}$). The mutation is a genetic operator used to maintain genetic diversity and to avoid local minima.

When the value of g is equal to the number of *epochs*, the iterative process stops and the imaginary axis ($\hat{\theta}$), which has the maximal accuracy estimator E_z in \mathbf{V} is selected.

Once the imaginary axis ($\hat{\theta}$) that maximizes class separability was found, the relevance of the 36 features in the analysis was verified. For this, the value of a specific feature is set to zero and the accuracy estimator (E_z^{new}) calculated. This process is repeated for each one of the available features. A feature is considered to be irrelevant to the discrimination when the difference between E_z and E_z^{new} is less than 1% of the value of E_z . Thus, the features that have an insignificant impact (i.e., relevance less than 1% of the accuracy estimator E_z) on the final discrimination of the groups are excluded from the analysis.

In the last step, the set of relevant features and the optimal projection axis are employed for the estimate of the *LDA-value* according to Eq. (10).

Description of the Parameters Employed for the Estimate of the LDA-Value

In this study the pattern vector was a 36-D feature vector, where each of its elements corresponds to one of the 18 computed features (listed in Table 4) from the tremor activity considering drawings of the spiral in both experimental conditions (i.e., OS and IS).

Once the imaginary axis ($\hat{\theta}$) that maximizes class separability was found, the relevance of the 36 features in analysis was verified. The features that had an insignificant impact on the final discrimination of the groups were excluded from the analysis. In total, seven features presented insignificant impact and were excluded. So, the set of relevant features employed for the estimate of the *LDA-value* totaled 29 features.

RESULTS

Young vs. Elderly Group

The results presented in this section take into account the analysis of the data collected from the young (G1–G2) and the elderly (G6–G7) groups. Table 2 lists the definition of these groups.

Figures 5a–5c show the mean and standard deviation obtained for each feature described in the Appendix for the young (G1–G2) and elderly groups (G6–G7), considering the outgoing and IS protocols. The analysis of variance (ANOVA) was applied for each protocol and feature. A probability value (p -value) less than 0.05 ($p < 0.05$) was considered as a threshold for significance analysis. A degree of freedom equal to 31 was used on the value of the statistic. The smallest value of p -value obtained across this series of statistical tests was lesser than 10^{-3} . Features that yielded significant differences between the groups are highlighted with an asterisk.

The LDA-Value

The results presented in this section take into account the analysis of the data collected from the seven groups (G1–G7). The correlation between the traditional features with the age of the subjects is shown in Table 3.

Even though some extracted features from the tremor activity yielded a significant correlation with age we estimate the *LDA-value* aiming to investigate a possible linear correlation between this feature and

TABLE 2. Characterization of the subjects from the young and elderly groups.

	Young (groups 1 and 2)	Elderly (groups 6 and 7)
Mean age (years)	29.4 ± 4.93	77.83 ± 3.97
Age range (years)	21–39	73–87
Number of subjects	20	12

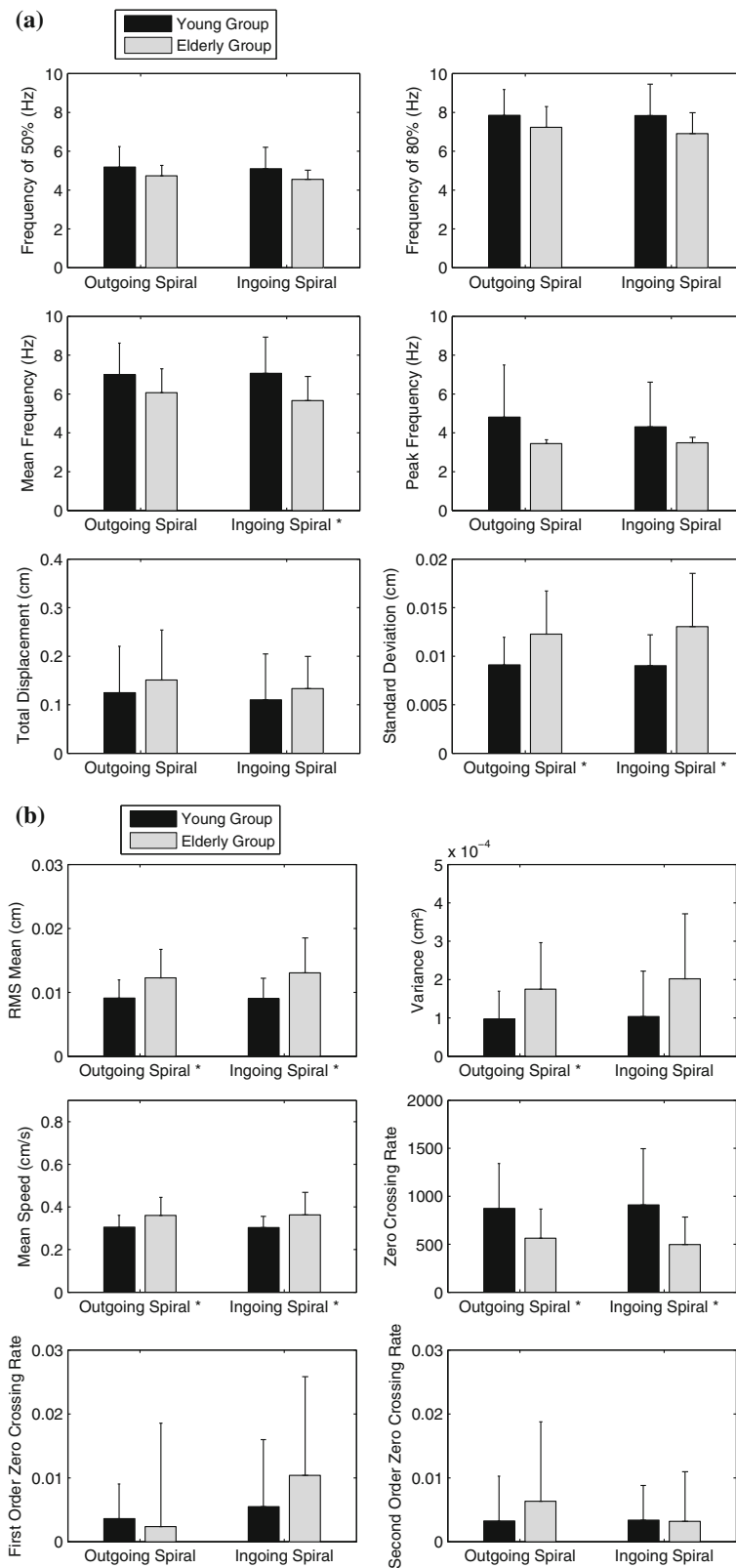


FIGURE 5. Mean values obtained for each feature and protocol (ingoing and OS). Error bars represent the standard deviation. The asterisks indicate those features that provided significant differences between the young and elderly groups. Note that in the case of the first- and second-order smoothness (c), statistical significance was found only for the IS protocol. As these features can characterize imperfections in the traces made by subjects it is possible to conclude that in general subjects from both the young and elderly groups presented more difficulty to draw the spiral toward its center.

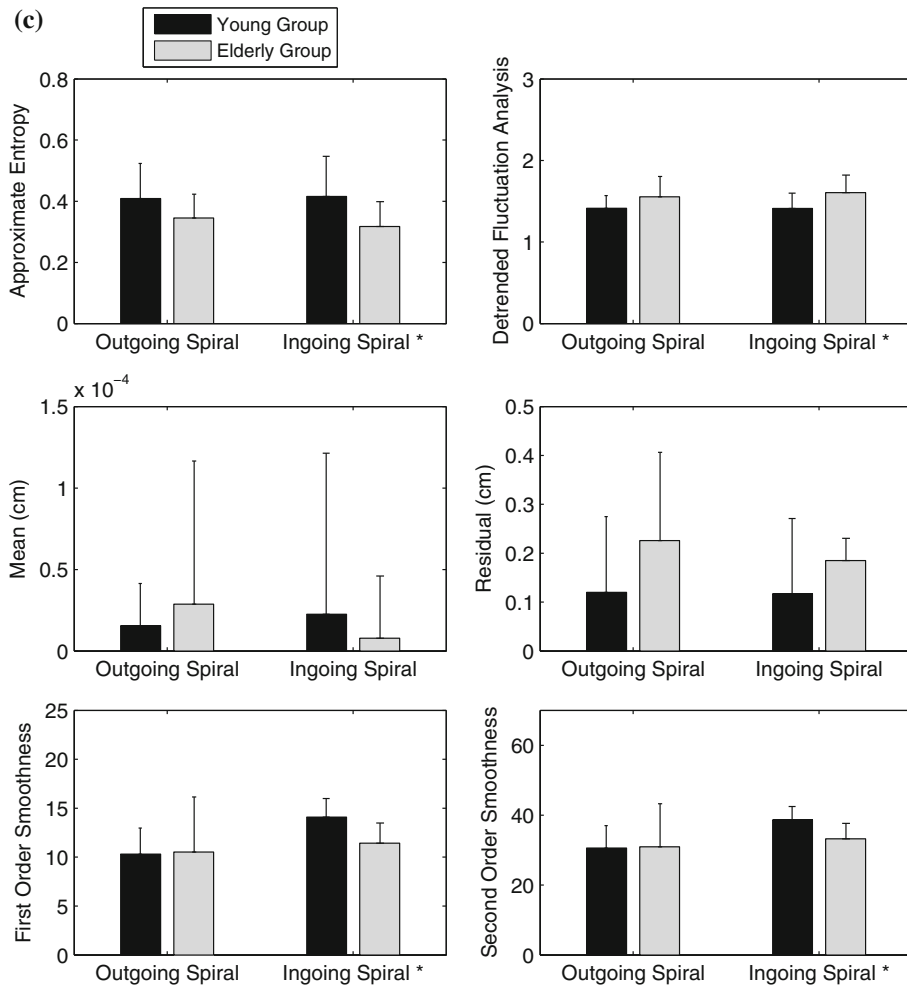


FIGURE 5. Continued.

age. In addition we verified the relevance of the traditional features on the estimate of the *LDA-value*.

In total, 29 features that are highlighted with an asterisk in Table 4 were identified as being relevant for the estimate of the *LDA-value*. The use of these features maximizes the separability between groups. Note that each feature can be applied in two conditions, i.e., OS and IS. The letters in this table are labels for each feature used in Eqs. (16)–(18). These equations resulted from the application of Eqs. (7)–(10).

$$r = \sqrt{a^2 + b^2 + c^2 + \dots + z^2 + A^2 + \dots + C^2} \quad (16)$$

$$\begin{aligned} \theta_1 &= \tan^{-1}\left(\frac{b}{a}\right); & \theta_2 &= \tan^{-1}\left(\frac{c}{\sqrt{a^2 + b^2}}\right); \\ \theta_3 &= \tan^{-1}\left(\frac{d}{\sqrt{a^2 + b^2 + c^2}}\right); & \dots; & \\ \theta_{28} &= \tan^{-1}\left(\frac{c}{\sqrt{a^2 + \dots + B^2}}\right) \end{aligned} \quad (17)$$

$$\begin{aligned} LDA\text{-value} &= 100 * r * \cos(\theta_1 + 1.54) * \cos(\theta_2 + 1.20) \\ &* \cos(\theta_3 + 1.70) * \cos(\theta_4 + 1.66) \\ &* \cos(\theta_5 + 3.10) * \cos(\theta_6 + 1.98) \\ &* \cos(\theta_7 + 0.70) * \cos(\theta_8 + 0.51) \\ &* \cos(\theta_9 + 2.69) * \cos(\theta_{10} + 0.74) \\ &* \cos(\theta_{11} + 0.90) * \cos(\theta_{12} + 1.17) \\ &* \cos(\theta_{13} + 0.99) * \cos(\theta_{14} + 1.64) \\ &* \cos(\theta_{15} + 1.85) * \cos(\theta_{16} + 1.05) \\ &* \cos(\theta_{17} + 0.92) * \cos(\theta_{18} + 0.93) \\ &* \cos(\theta_{19} + 1.21) * \cos(\theta_{20} + 2.26) \\ &* \cos(\theta_{21} + 0.72) * \cos(\theta_{22} + 1.68) \\ &* \cos(\theta_{23} + 1.44) * \cos(\theta_{24} + 2.25) \\ &* \cos(\theta_{25} + 1.55) * \cos(\theta_{26} + 1.25) \\ &* \cos(\theta_{27} + 1.63) * \cos(\theta_{28} + 1.69) \end{aligned} \quad (18)$$

TABLE 3. Correlation between the traditional features and the age of subjects.

Feature	Correlation coefficient		ANOVA p -value	
	OS	IS	OS	IS
Frequency of 50%	-0.152	-0.195		
Frequency of 80%	-0.137	-0.197		
Mean frequency*	-0.178	-0.272		<0.05
Peak frequency	-0.222	-0.241		
TD	0.008	0.092		
Standard deviation*	0.213	0.272		<0.05
Approximate entropy*	-0.175	-0.279		<0.05
First-order smoothness*	0.028	-0.409		< 10^{-2}
DFA*	0.195	0.294		<0.05
Mean	-0.029	0.034		
Residual*	0.139	0.271		<0.05
RMS mean*	0.213	0.272		<0.05
Second-order smoothness*	0.035	-0.398		< 10^{-2}
Variance	0.207	0.232		
MS	0.192	0.197		
Zero crossing rate	-0.164	-0.195		
First-order zero crossing	-0.087	0.127		
Second-order zero crossing	0.046	0.056		

Features that presented a significant difference between the groups are highlighted with (*) and in this case the estimated p -value of the statistical test is shown.

TABLE 4. Relevant features for the estimate of the LDA -value.

Feature	OS	IS
Frequency of 50%	*(a)	
Frequency of 80%	*(b)	*(s)
Mean frequency	*(c)	
Peak frequency	*(d)	*(t)
TD	*(e)	*(u)
Standard deviation	*(f)	
Approximate entropy	*(g)	
First-order smoothness	*(h)	*(v)
DFA	*(i)	
Mean	*(j)	*(w)
Residual	*(k)	*(x)
RMS mean	*(l)	*(y)
Second-order smoothness	*(m)	*(z)
Variance	*(n)	*(A)
MS	*(o)	*(B)
Zero crossing rate	*(p)	
First-order zero crossing	*(q)	
Second-order zero crossing	*(r)	*(C)

The most relevant features are highlighted with **. The letters in brackets are feature labels used in Eqs. (16) and (17).

Figure 6 depicts the LDA -values obtained for the seven groups. A visual inspection of the box plots allows for the conclusion that the LDA -value is a feature whose value increases with age.

When estimating the correlation between the LDA -value and age, we obtained a Pearson's correlation

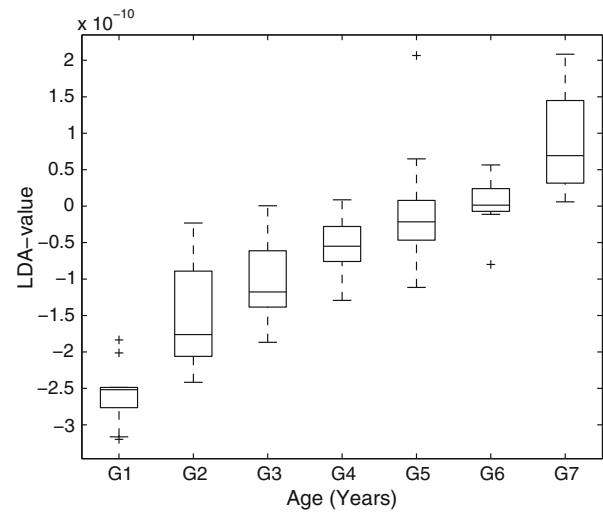


FIGURE 6. Box plot of the LDA -value for the seven groups. The cross sign (+) in the graph represents the outliers. The solid lines in the boxes are the median LDA -value for the groups. These results show that an increase in the age range of the studied groups is followed by an increase in the LDA -value.

coefficient equal to 0.83, indicating a high degree of correlation between these variables. The ANOVA statistical test was applied to the LDA -value data, and the p -values are shown in Table 5 whenever statistical significance was found. These values indicate that the LDA -value provided significant differences for most groups.

Figure 7 shows a linear fit obtained through the relation between age and the LDA -value. The analysis of the parameters of the linear model (see Table 6) shows that there is a linear trend between the two variables.

DISCUSSION

The Analysis of the Young and Elderly Groups

From the analysis of Fig. 5 it is possible to conclude that the features that provided a significant difference between the two groups, for the OS and IS protocols, are mean frequency (IS), standard deviation (OS and IS), approximate entropy (IS), detrended fluctuation analysis (DFA) (IS), first-order smoothness (IS), second-order smoothness (IS), root mean square (RMS) mean (OS and IS), variance (OS), mean speed (MS) (OS and IS), zero crossing rate (OS and IS).

As the values obtained for the mean frequency and zero crossing rate decreased in the elderly group, it is possible to conclude that the oscillation of tremor activity in the elderly group is slower than in the young group.

TABLE 5. ANOVA p -values for the LDA -value.

	Group 1	Group 2	Group 3	Group 4	Group 5	Group 6
Group 1	×					
Group 2	$<10^{-2}$	×				
Group 3	$<10^{-5}$		×			
Group 4	$<10^{-7}$	$<10^{-2}$		×		
Group 5	$<10^{-6}$	$<10^{-3}$	<0.05		×	
Group 6	$<10^{-9}$	$<10^{-4}$	$<10^{-2}$	<0.05		×
Group 7	$<10^{-6}$	$<10^{-3}$	$<10^{-3}$	$<10^{-2}$	<0.05	<0.05

Statistical significant p -values are shown for each pair of groups.

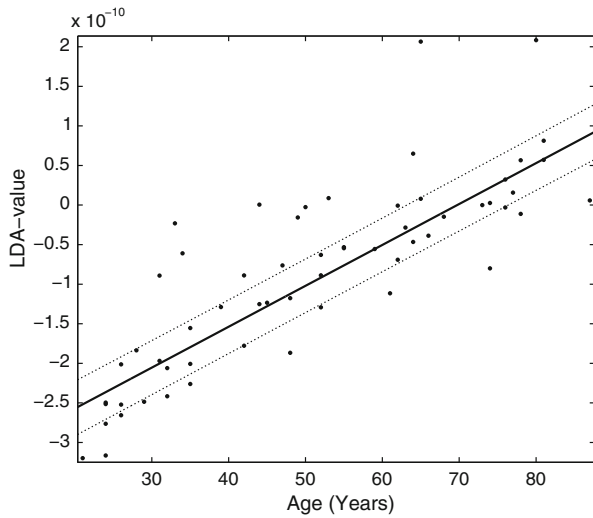


FIGURE 7. Linear model fitted to the LDA -values shown in Fig. 6. The dotted lines are the 95% confidence interval bounds. The parameters of the linear model are shown in Table 6 and their analysis suggests that this type of model is adequate for representing the relation between the two variables (i.e., the LDA -values and age).

Moreover, the values of RMS, variance, and standard deviation show that the elderly group had larger displacement amplitude of the tremor activity. As in probability theory the variance of a random variable is a measure of statistical dispersion and the results show that the elderly group presented a larger value of variance (see Fig. 5b), it is possible to conclude that the distribution of the tremor activity from the elderly group is more spread out than that of the young group.

The MS values were smaller for the young group and, consequently, the total displacement (TD) of the tremor activity was larger in the elderly group.

Additionally, through the analysis of the DFA and approximate entropy, we can observe a change in the randomness of the signal, i.e., the tremor activity from the elderly group has higher predictability than that obtained for the young group as suggested by the increase in the DFA coefficients and the reduction of the entropy values.

TABLE 6. Parameters of the linear model.

$f(x) = p1*x + p2$	Mean = 50.86
x is normalized by:	SD = 18.93
Coefficients (with 95% confidence bounds)	
$p1 = 9.782 \times 10^{-11}$ (9.342×10^{-11} , 1.022×10^{-10})	
$p2 = -9.758 \times 10^{-11}$ (-1.019×10^{-10} , -9.322×10^{-11})	
Goodness of fit	
SSE = 1.598×10^{-20}	
$R^2 = 0.9803$	
Adjusted $R^2 = 0.98$	
RMSE = 1.674×10^{-11}	

The analysis of the features first-order smoothness and second-order smoothness in Fig. 5c allows us to conclude that in general subjects from both the young and elderly groups presented more difficulty to draw the spiral toward its center. This is based on the fact that these features can characterize imperfections in the traces made by subjects, i.e., the larger their amplitudes the more imperfect the trace is. The results depicted in Fig. 5c support this assumption by showing an increase in the feature amplitudes for both groups.

On the Use of the LDA -Value

Although the statistical analysis showed that some of the traditional investigated features provided the discrimination between the young and elderly groups as reported in other studies^{11,25,33} none of them showed to be linearly correlated with age as suggested by the obtained correlation coefficients presented in Table 3, which means that a linear model is not suitable to describe the relation between each one of those features and age.

This was the main motivation to seek an alternative feature that could describe the relationship between physiological kinetic tremor and age. In this context, a modified version of LDA, where the rotation of the projection axes is carried out by means of a procedure based on GA, was applied to estimate the LDA -value,⁷ which in the context of this research is a one-dimensional feature obtained by the linear combination of the studied traditional features. The LDA -value was able to discriminate the elderly (G6–G7) from the young (G1–G7) groups as shown in the result presented in Fig. 6, and also to characterize a linear relationship with age as depicted in Fig. 7 and supported by the parameters of the linear model given in Table 6. Such relationship has not been described in the literature for the study of physiological kinetic tremor.

The results also allowed us to verify that the LDA -value is a relevant feature for kinetic tremor analysis, with potential application in a number of correlated studies in areas such as Physiotherapy, Neurology,

Geriatrics, and others. As the *LDA-value* showed to be linearly correlated with age for the group of clinically healthy subjects, it is possible that this correlation is not valid for patients with pathological tremor. In this case this parameter could potentially be employed for the discrimination between physiological and pathological tremor.

This study cannot completely answer the question of how we can use the *LDA-value* to characterize the degree of tremor *per se* because the collected signals, which are basically kinetic measures extracted from the spiral movement, could be composed of a number of variables (e.g., intermittent path corrections) that could be correlated with age. Further studies should be carried out to verify the hypothesis of correlation between tremor and the *LDA-value*. For this, the experimental protocol should take into account static and dynamic conditions. A possible approach could be the use of low-*g* accelerometers (e.g., MMA2260, Freescale) for measuring tremor. Subjects could follow a spiral drawn in a board by using a laser pointer for the dynamic condition, whereas for the static condition they could point to a specific target for a given period of time. The results of the *LDA-value* obtained from these two conditions could be contrasted to those obtained in this study.

Recent studies have discussed the classification of physiological tremor.²² A possible criterion for tremor categorization is to take into account the underlying processes related to its origins.²² For instance, motion tremor, which was the object of study in this research, is believed to be mainly driven by a peripheral manifestation of central rhythmic activity whereas postural tremor may be related to both central and peripheral processes.²² Note that both motion and postural tremor, and also other types of tremor (e.g., rest tremor), may be classified as physiological tremor,²² and they may be correlated with age.

The results found in our study suggest a degradation of the motor control with age under a specific task. Considering the hypothesis that tremor may be a manifestation in the periphery due to oscillatory neural activity in the central nervous system²² and that such activity has a role in motor control, the analysis of tremor introduced in this study, i.e., the use of the *LDA-value* estimated from tremor activity, may be seen as an investigative tool which provides a non-invasive way of studying the rhythmic nature of human motor control.²²

CONCLUSIONS

In this study, different from other researches, we addressed the issues of quantifying physiological-kinetic

tremor and of studying its correlation with age. For this, we investigated the tremor activity obtained from distinct groups of subjects. The subjects were grouped into classes according to their age. In the first analysis we verified significant differences between the young and elderly groups.

In the second analysis, LDA was introduced as a new method to analyze tremor activity through the study of hand-drawn patterns by using a digitizing tablet. Our results indicate that the *LDA-value* was effective in the quantification of kinetic tremor showing a high degree of correlation (0.83) with age. As the *LDA-value* is linearly correlated with age, this index may have great importance in future research, in particular in those related to the discrimination between physiological and pathological tremors.

Normal aging is associated with a decline in the functional capacity of the neuromuscular system, which is associated with an increase in the amplitude of physiological tremor. This situation may have severe implications in the ability of any individual to perform everyday tasks that require fine motor skills.

The analysis of physiological kinetic tremor of individuals may be an important tool for the characterization of physiological tremor. In this context, this study introduced a new feature which showed to be correlated with the age of subjects. As this feature is in a single dimensional space it can be easily interpreted and visualized. Furthermore, the analysis of this feature may be evaluated in the context of the patient's history and correlated with neurological exams and potentially be used in the discrimination between physiological and pathological tremors. The early diagnosis of a pathological tremor can lead to appropriate treatment, which can provide a better condition of life for individuals.

The main limitation of the obtained results is with regard to the number of studied subjects, specifically, it was difficult to recruit individuals aged over 80 years old in our community, during the period of the research, that met the requirements of the experimental protocol, i.e., in good neurological conditions and without taking drugs that could stress or reduce tremor. Despite this limitation, this research introduced a new way of analyzing kinetic tremor activity for the characterization of physiological tremor.

APPENDIX

This appendix describes the traditional set of features employed in the data analysis.

Frequency Domain Features

From the power spectrum S_x of the signal, obtained from the Fourier transform, the following features were estimated:

1. *Mean frequency*: it is the expected value of S_x as defined in Eq. (19).

$$f_{\text{mean}} = \frac{\sum_{i=1}^N (S_x(i) * f(i))}{\sum_{i=1}^N S_x(i)} \quad (19)$$

where f_{mean} is the mean frequency, N the number of frequency bins in the spectrum, $f(i)$ the frequency of the spectrum at bin i , and $S_x(i)$ is the intensity of the spectrum at bin i .

2. *Peak frequency*: it is the frequency for which S_x is maximal.
3. *Frequency of 50%*: it is also known as the median frequency. It is the frequency that divides the area under S_x into two equal parts.
4. *Frequency of 80%*: it is the frequency for which 80% of the total energy of S_x is below it.

Detrended Fluctuation Analysis

DFA is a tool for analysis of random signals that estimates the α exponent which may characterize the nature of the time-series.^{9,26} The steps to estimate the value of the α exponent are provided below.

The discrete time-series $S(n)$, $n = 0, \dots, N - 1$, where N is the number of samples, is divided into K intervals, of τ samples each, without overlapping. For each interval K , $K = 0, \dots, N - 1$, the mean value \overline{S}_k (Eq. 20), the parameter y_k (Eq. 21) and the linear model $z_k(i)$ (Eq. 22) are calculated, where a and b are the angular and linear coefficients of the linear model, respectively, for k th interval.

$$\overline{S}_k = \frac{1}{\tau} \sum_{i=k\tau}^{k\tau-1} S(i) \quad (20)$$

$$y_k = \sum_{i=k\tau}^{k\tau-1} (S(i) - \overline{S}_k) \quad (21)$$

$$z_k(i) = ai + b, \quad k\tau \leq i \leq k\tau - 1 \quad (22)$$

The fluctuation function FF_k for each interval k is calculated by Eq. (23). Then the mean value of FF_k for all intervals is estimated as in Eq. (24).

$$FF_k = \sqrt{\frac{1}{\tau} \sum_{i=k\tau}^{k\tau-1} |y_k - z_k(i)|^2} \quad (23)$$

$$F_k = \frac{1}{K} \sum_{k=0}^{K-1} FF_k \quad (24)$$

A behavior $F_k \sim \tau^\alpha$ is expected, where the characteristic exponent (α) can be extracted through the inclination of the straightline in the graph $\log(F_k)$ vs. $\log(\tau)$. The interpretation of the exponent α is as follows: if the exponent (α) is less than 0.5 characterizes an anti-persistent signal; α larger than 0.5 characterizes a persistent signal; and a white noise has an exponent (α) equal to 0.5.

Mean Speed

The MS of the tremor activity is the average of the instantaneous velocity $v(n)$ as given in Eqs. (25) and (26), where, n is the discrete time and T the period, which is the inverse of the sampling frequency.

$$MS = \frac{1}{N-1} \sum_{i=0}^{N-1} v(i) \quad (25)$$

$$v(n) = \frac{|S(n+1) - S(n)|}{T} \quad (26)$$

Total Displacement

The TD of the tremor activity is calculated by summing up all the distances from two consecutive samples, as shown in Eq. (27).

$$TD = \sum_{i=0}^{N-1} |S(i+1) - S(i)| \quad (27)$$

RMS Mean

Also known as quadratic mean, the RMS is a statistical measure of the magnitude of a varying quantity, and it can be calculated by using Eq. (28).

$$RMS = \sqrt{\frac{\sum_{i=0}^{N-1} (S(i))^2}{N-1}} \quad (28)$$

Approximate Entropy

Approximate entropy (*ApEn*) is a tool used to quantify the regularity of a signal.²⁷ It is usually normalized between 0 and 2, where 0 represents a predictable signal (e.g., sinusoidal signal) and 2 an unpredictable signal (e.g., a white noise).

In order to calculate the approximate entropy of the time-series $S(n)$ it is necessary to select values for the parameters w and μ , where w is the length of a pattern, and μ is the criterion of similarity or the tolerance for pattern comparison. If a signal window of w samples beginning at sample i is denoted by $p_w(i)$, then two patterns $p_w(i)$ and $p_w(j)$ will be similar if the difference between any pair of corresponding measures of the patterns is less than μ , therefore, $[S(i + l) - S(j + l)] < \mu$, for $0 \leq l < w$.

Being P_w the set of all patterns of length w in $S(n)$, $C_{iw}(\mu)$ is the number of patterns in P_w that are similar to $p_w(i)$. In this case, $C_{iw}(\mu)$ can be calculated for each pattern in P_w , setting up $C_w(\mu)$ as the average of these values. $C_w(\mu)$ measures the regularity or the frequency of similar patterns to a certain pattern in $S(n)$, with a window length equal to m , obeying the tolerance μ . Therefore, the approximate entropy of $S(n)$ can be defined as in Eq. (29).

$$ApEn(w, \mu, S(n)) = \ln \left[\frac{C_w(\mu)}{C_{w+1}(\mu)} \right] \quad (29)$$

The $ApEn$ measures the similarity between patterns $p_w(i)$ and $p_w(j)$. This technique was applied to the tremor signal with a value of w equal to 2 and the value of μ equal to $0.2SD(S(n))$, where $0.2SD(S(n))$ is the standard deviation of $S(n)$, as suggested by Pincus.²⁷

First-Order Smoothness

This tool can characterize imperfections in spirals drawn by the subjects. The calculation of this feature is based on the overall deviation of the spiral, in such a way that an ideal spiral results in a value of the first-order smoothness equal to zero. It happens because, in this case, there is a constant rate of change in the values of the spiral. Thus, it can be concluded that the larger the value of the first-order smoothness, the larger will be the deviation from the drawn spiral with respect to a given template.²⁸

The first-order smoothness can be calculated through the divergence of all $\Delta r/\Delta\theta$, where Δr is the difference between the ideal spiral's radius and that resultant from the spiral drawn by subjects and $\Delta\theta$ is the difference between the ideal spiral's angle and that resultant from the spiral drawn by subjects. This feature is calculated by Eq. (30).

$$\text{First-order smoothness} = \ln \left[\frac{1}{\theta} \sum \left(\frac{\Delta r}{\Delta\theta} - \bar{r}_\theta \right)^2 \right] \quad (30)$$

where θ is the total angle over which the spiral is drawn and \bar{r}_θ is the RMS value of $\Delta r/\Delta\theta$.

Second-Order Smoothness

The second-order smoothness can be defined as the rate of change of first-order smoothness. This feature can be calculated through the first derivative of first-order smoothness. Equation (31) shows how second-order smoothness is calculated.

$$\text{Second-order smoothness} = \ln \left[\frac{1}{\theta} \sum \left(\frac{\Delta \Delta r}{\Delta\theta} - d\bar{r}_\theta \right)^2 \right] \quad (31)$$

where $d\bar{r}_\theta$ is the derivative of the RMS $\Delta r/\Delta\theta$ value.²⁸

First-Order Zero Crossing Rate

This feature is a measure of irregularity of the signal and shows how frequently $\Delta r/\Delta\theta$ values cross their own RMS value. The first-order zero crossing rate (FOZCR) is more sensitive to small or frequent fluctuations. Equation (32) shows the calculation of this feature, where N is the total number of data points in the time series, i is a specific data point in time series, \bar{r}_θ is the RMS value of $\Delta r/\Delta\theta$.²⁸

The $\text{sign}(x)$ function works in such a way that:

- If $x > 0$, then $\text{sign}(x) = 1$
- If $x = 0$, then $\text{sign}(x) = 0$
- If $x < 0$, then $\text{sign}(x) = -1$

$$\text{FOZCR} = \left[\frac{1}{2(N-1)} \sum_{i=1}^{N-1} \left[\text{sign} \left\{ \left(\frac{\Delta r}{\Delta\theta} \right)_{i+1} - \left(\frac{\Delta r}{\Delta\theta} \right)_{\bar{r}_\theta} \right\} \right] - \left[\text{sign} \left\{ \left(\frac{\Delta r}{\Delta\theta} \right)_i - \left(\frac{\Delta r}{\Delta\theta} \right)_{\bar{r}_\theta} \right\} \right] \right] * 100\% \quad (32)$$

Second-Order Zero Crossing Rate

This feature is the rate of change of the first-order zero crossing rate, i.e., first derivative. The second-order zero crossing rate (SOZCR) provides valuable additional information concerning how regularly irregular or irregularly irregular a given spiral is. This feature can be calculated by Eq. (33), where \bar{r}_θ is the RMS value of change in radius vs. angle.²⁸

$$\text{SOZCR} = \left[\frac{1}{2(N-1)} \sum_{i=1}^{N-1} \left[\text{sign} \left(\frac{\Delta \Delta r}{\Delta\theta} \right) \right] (i+1) - (d\bar{r}_\theta) \right] - \left[\text{sign} \left(\frac{\Delta \Delta r}{\Delta\theta} \right) \right] (i) - (d\bar{r}_\theta) \right] * 100\% \quad (33)$$

Residual

This feature reflects the total distance between the spiral after the process of linearization and a line of best fit on the radius vs. angle graph. The larger this value is the more spiral changes its shape in an irregular way. This can be called RMS of r (radius) and it can be calculated by using Eq. (34), where Δr is the radius divergence of each point of the linearized digitizing tablet signal from the line of best fit, that represents the ideal spiral.²⁸

$$\text{Residual} = \sqrt{\frac{\sum_{i=1}^N (\Delta r_1)^2 + (\Delta r_2)^2 + (\Delta r_3)^2 + \dots + (\Delta r_N)^2}{N-1}} \quad (34)$$

ACKNOWLEDGMENT

The authors would like to thank the Brazilian government for supporting this study (Project PPSUS/FAPEMIG 2006 Nr. 3300/06).

REFERENCES

- ¹Albers, J. W., A. R. Potvin, W. W. Tourtellotte, R. W. Pew, and R. F. Stribley. Quantification of hand tremor in the clinical neurological examination. *IEEE Trans. Biomed. Eng.* BME-20:27–37, 1973.
- ²Benito-Leon, J., F. Bermejo-Pareja, E. D. Louis, and for the Neurological Disorders in Central Spain Study Group. Incidence of essential tremor in three elderly populations of central Spain. *Neurology* 64:1721–1725, 2005.
- ³Bermejo-Pareja, F., E. D. Louis, J. Benito-León, and for the Neurological Disorders in Central Spain Study Group. Risk of incident dementia in essential tremor: a population-based study. *Mov. Disord.* 22:1573–1580, 2007.
- ⁴Bhagwath, G. Tremors in elderly persons: clinical features and management. *Hosp. Physician* 49:31–49, 2001.
- ⁵Borges, V., and H. B. Ferraz. Tremors. *Rev. Neurosci.* 14:43–47, 2006.
- ⁶Burke, E. K., J. P. Newall, and R. F. Weare. A Memetic Algorithm for University Exam Timetabling. Selected papers from the First International Conference on Practice and Theory of Automated Timetabling. Springer-Verlag, pp. 241–250, 1996.
- ⁷Cavalheiro, G., M. F. S. Almeida, A. Pereira, and A. O. Andrade. Study of age-related changes in postural control during quiet standing through Linear Discriminant Analysis. *Biomed. Eng. Online* 8, 2009.
- ⁸De Lima, E., A. O. Andrade, J. Pons, P. Kyberd, and S. Nasuto. Empirical mode decomposition: a novel technique for the study of tremor time series. *Med. Biol. Eng. Comput.* 44:569–582, 2006.
- ⁹Delignieres, D., T. Deschamps, A. Legros, and N. Caillou. A methodological note on nonlinear time series analysis: Is the open- and closed-loop model of Collins and De Luca (1993) a statistical artifact? *J. Mot. Behav.* 35:86–96, 2003.
- ¹⁰Deuschl, G., M. Lauk, and J. Timmer. Tremor classification and tremor time series analysis. *Chaos* 5:48–51, 1995.
- ¹¹Elble, R. J. Characteristics of physiologic tremor in young and elderly adults. *Clin. Neurophysiol.* 114:624–635, 2003.
- ¹²Elble, R. J., M. Brilliant, K. Leffler, and C. Higgins. Quantification of essential tremor in writing and drawing. *Mov. Disord.* 11:70–78, 1996.
- ¹³Elble, R. J., S. L. Pullman, J. Y. Matsumoto, J. Raethjen, G. Deuschl, and R. Tintner. Tremor amplitude is logarithmically related to 4- and 5-point tremor rating scales. *Brain* 129:2660–2666, 2006.
- ¹⁴Elble, R. J., R. Sinha, and C. Higgins. Quantification of tremor with a digitizing tablet. *J. Neurosci. Methods* 32:193–198, 1990.
- ¹⁵Feys, P., W. Helsen, A. Prinsmel, S. Ilsbrouckx, S. Wang, and X. Liu. Digitised spirometry as an evaluation tool for intention tremor in multiple sclerosis. *J. Neurosci. Methods* 160:309–316, 2007.
- ¹⁶Kim, H.-C., D. Kim, and S. Y. Bang. Extensions of LDA by PCA mixture model and class-wise features. *Pattern Recogn.* 36:1095–1105, 2003.
- ¹⁷Liu, X., C. B. Carroll, S.-Y. Wang, J. Zajicek, and P. G. Bain. Quantifying drug-induced dyskinesias in the arms using digitised spiral-drawing tasks. *J. Neurosci. Methods* 144:47–52, 2005.
- ¹⁸Louis, E. D., B. Ford, S. Frucht, and R. Ottman. Mild tremor in relatives of patients with essential tremor: what does this tell us about the penetrance of the disease? *Arch. Neurol.* 58:1584–1589, 2001.
- ¹⁹Louis, E. D., B. Ford, S. Frucht, D. Rabinowitz, and R. Ottman. Evidence for familial aggregation of tremor in normal individuals. *Neurology* 57:110–114, 2001.
- ²⁰Louis, E. D., K. J. Wendt, S. L. Pullman, and B. Ford. Is essential tremor symmetric? observational data from a community-based study of essential tremor. *Arch. Neurol.* 55:1553–1559, 1998.
- ²¹Mansur, P. H. G., L. K. P. Cury, A. O. Andrade, A. A. Pereira, G. A. A. Miotto, A. B. Soares, and E. L. M. Naves. A review on techniques for tremor recording and quantification. *Crit. Rev. Biomed. Eng.* 35:343–362, 2007.
- ²²McAuley, J. H., and C. D. Marsden. Physiological and pathological tremors and rhythmic central motor control. *Brain* 123:1545–1567, 2000.
- ²³Mergl, R., P. Tigges, A. Schröter, H.-J. Möller, and U. Hegerl. Digitized analysis of handwriting and drawing movements in healthy subjects: methods, results and perspectives. *J. Neurosci. Methods* 90:157–169, 1999.
- ²⁴Miralles, F., S. Tarongí, and A. Espino. Quantification of the drawing of an Archimedes spiral through the analysis of its digitized picture. *J. Neurosci. Methods* 152:18–31, 2006.
- ²⁵Morrison, S., P. Mills, and R. Barrett. Differences in multiple segment tremor dynamics between young and elderly persons. *J. Gerontol. A Biol. Sci. Med. Sci.* 61:982–990, 2006.
- ²⁶Norris, J. A., A. P. Marsh, I. J. Smith, R. I. Kohut, and M. E. Miller. Ability of static and statistical mechanics posturographic measures to distinguish between age and fall risk. *J. Biomech.* 38:1263–1272, 2005.
- ²⁷Pincus, S. M. Approximate entropy as a measure of system complexity. *Proc. Natl Acad. Sci. USA* 88:2297–2301, 1991.
- ²⁸Pullman, S. L. Spiral analysis: a new technique for measuring tremor with a digitizing tablet. *Mov. Disord.* 13:85–89, 1998.
- ²⁹Raethjen, J., F. Pawlas, M. Lindemann, R. Wenzelburger, and G. Deuschl. Determinants of physiologic tremor in a

- large normal population. *Clin. Neurophysiol.* 111:1825–1837, 2000.
- ³⁰Rudzińska, M., A. Izworski, K. Banaszekiewicz, S. Bukowczan, M. Marona, and A. Szczudlik. Quantitative tremor measurement with the computerized analysis of spiral drawing. *Pol. J. Neurol. Neurosurg.* 41:510–516, 2007.
- ³¹Shin, K.-S., and Y.-J. Lee. A genetic algorithm application in bankruptcy prediction modeling. *Expert Syst. Appl.* 23:321–328, 2002.
- ³²Smaga, S. Tremor. *Am. Fam. Physician* 68:1545–1553, 2003.
- ³³Sturman, M. M., D. E. Vaillancourt, and D. M. Corcos. Effects of aging on the regularity of physiological tremor. *J. Neurophysiol.* 93:3064–3074, 2005.
- ³⁴Timmer, J., M. Lauk, W. Pflieger, and G. Deuschl. Cross-spectral analysis of physiological tremor and muscle activity. *Biol. Cybern.* 78:359–368, 1998.
- ³⁵Ulmanová, O., C. N. Homann, R. Ulman, R. Jech, V. Capek, J. Klempír, and E. Ruzicka. Tremor magnitude: a single index to assess writing and drawing in essential tremor. *Parkinsonism Relat. Disord.* 13:250–253, 2007.
- ³⁶Wenzelburger, R., J. Raethjen, K. Löffler, H. Stolze, M. Illert, and G. Deuschl. Kinetic tremor in a reach-to-grasp movement in Parkinson's disease. *Mov. Disord.* 15:1084–1094, 2000.
- ³⁷Wright, A. Genetic algorithms for real parameter optimization. In: *Foundations of genetic algorithms*, edited by G. Rawlins. San Mateo, CA: Morgan Kaufmann, 1991, pp. 205–218.